Proceeding of the IEEE
International Conference on Robotics and Biomimetics
Dali, China, December 2019

# A New Method For Fiber Bragg Grating Based Needle Shape Sensing Calibration*

LeiFeng Zhang, ChangLe Li, XueHe Zhang, GangFeng Liu, YuBin Liu,
Jie Zhao, Guang Ban and YiLun Fan

*State Key Laboratory of Robotics and System*
*Harbin Institute of Technology*
*Harbin 150080, NO. 2, YiKuang Street, NanGang District Harbin City, HeiLongJiang Province, China*

leifeng_zhang@yeah.net
{lichangle, zhangxuehe, liugangfeng, liuyubin & jzhao}@hit.edu.cn
b_guang@163.com, 1246371494@qq.com

***Abstract* - Accurate placement of the needle is critical in percutaneous surgery. Needle shape reconstruction technology based on fiber Bragg gratings (FBGs) sensor is considered to have the potential to achieve this goal. In this paper, we present a temperature-insensitive calibration model for calibrating needles with FBG sensors to accurately estimate its deformation. In addition, we have designed a device for simultaneously calibrating the loading direction and shape. Preliminary results indicate that the proposed model is theoretically insensitive to temperature, but in fact it can only be used within a certain temperature range. The resolution of the loading direction increases as the degree of bending increases, with a maximum error of 8.58°. Shape reconstruction error can be less than 1.5mm with small needle bending. This calibration method can meet clinical applications.**

***Index Terms* -. *percutaneous surgery, shape sensing, fiber Bragg gratings (FBGs), calibration***

## I. INTRODUCTION

Percutaneous fine needle insertion is widely used in minimally invasive medical applications such as biopsy, brachytherapy, and drug injection [1]. In particular, percutaneous radioactive seed implantation has been used more and more in clinical practice in recent years to greatly improve the survival rate of patients with cervical cancer and prostate cancer [1, 2]. In order to improve the accuracy of biopsy and particle implantation, a lot of research about robot-assisted percutaneous fine needle insertion surgery have been done [3, 4]. However, due to the problem that the needle used for particle implantation is easy to bend, its effect in some scenes is not satisfactory, such as the maxillofacial with rich blood vessels and nerves [5]. The deflection of the needle body is mainly caused by the uneven force of the bevel tip of needle and the anisotropy of human tissue [6, 7]. Currently, only a handful of experienced doctors can estimate the deflection of the needle according to the feel and experience under the guidance of CT or ultrasound to avoid some important anatomical structures. CT can provide high resolution and low noise images to show the position and deformation of the needle. However, it is difficult to track the needle tip and needle deformation in real time because of the increase in the patient's radiation exposure. Although ultrasound is harmless to the human but the image quality is poor, it is difficult to precisely track the position of the needle. Therefore, it is extremely difficult to monitor the deformation of the needle in real time through the existing medical means. In such case, it is necessary to develop a new medical device real-time feedback pin shape change.

Previously many researchers and manufacturers have proposed a variety of real-time monitoring of needle shape solutions through the addition of sensors. Among them, the most widely used is six-degree-of-freedom electromagnetic tracking solution from NDI (Northern Digital Inc). Attaching multiple sensors to the inside of the trocar allows the needle to be positioned and shaped in real time. The smallest of the products it offers is only 0.56mm in diameter and is the most current product that best meets clinical needs. It's problem is that the electromagnetic generator must be kept at a small distance (<20cm) from the sensor to maintain high accuracy, so it is very easy to interfere with the doctor's operation. Some researchers have proposed installing a six-dimensional torque/force sensor at the end of the needle to estimate the needle shape through changes in the force signal [8]. Although some results have been achieved, the large noise of force/torque leads to poor estimation of needle shape especially the deformation is small. With the development of optical fiber technology, some researchers have tried to apply FBG (Fiber Bragg grating) sensors to the shape detection of needles in recent years considering the advantages of these sensors: high accuracy, fast response, bio-compatible, robustness and small size [9-11]. Its basic principle of measuring needle deformation is the plane hypotheses in the deformation of elastic beams. A more popular solution is to attach three optical fibers with two or more FBGs to each other at 120 degrees on the inner stylet of the trocar with the fine grooves [12]. Since the optical fiber is attached to the edge of the needle, the bending of the needle causes the optical

* This work is supported by the National Natural Science Foundation of China (NSFC) (Grant no. U1713202, 61803126) · National High-tech R&D Program of China (No. 2017YFB1303600 ) and DongGuan Major Special Project(no. 201721502011).



978-1-7281-6321-5/19//$31.00 ©2019 IEEE

fiber to be subjected to tensile stress or compressive stress, thereby causing the grating reflection wavelength to move forward or backward. Analyze the offset of the three grating wavelengths at a location to calculate the curvature and direction of the bend. There are some researchers have done a lot of work on FBG grating in needle shape perception. Previous studies have proposed three shape calculation methods: 1) based on geometry[13]; 2) based on calibration matrix and 3) based on Lie group theory[11, 14, 15]. However, each calculation method must be calibrated before use to obtain the relationship between the FBG wavelength shift and the curvature of the needle deformation. There are two proposed calibration methods include template-based methods and load-based methods[15, 16]. The template-based method is to place the needle into a template engraved with a groove of a certain shape to obtain the relationship between the curvature at the position of the measurement point (location of FBG) and the wavelength shift. This method has a high calibration accuracy but cannot calibrate the deflection direction of the needle. The load-based method is to deform the needle by applying a certain load, and then obtain the shape by image processing or electromagnetic tracking to finish calibration. This method is capable of simultaneously calibrating the direction and curvature but is less accurate due to the errors from the needle shape acquisition process.

Therefore, the purpose of this study is to propose a method for simultaneously calibrating the direction and curvature with high precision. The proposed method includes a new device and an algorithm for simultaneously calibrating loading direction and curvature based on the least squares. This method can further improve the accuracy of the perception of needle deformation and promote the application of this special medical device in robotic assisted surgery.

This paper is organized as follows. First, the method proposed is explained in Section II, including the needle configuration and calibration algorithm. In Section III we experiments on calibration and test calibration result. Then we present the test results on the needle shape determination in Section IV. Section V is the conclusion and recommendations for future work.

## II. METHODS

### A. Fiber Bragg Grating sensors

An FBG sensor reflect a certain wavelength of light (Bragg wavelength $\lambda_B$), which is calculated as

$$\lambda_B = 2n_{eff}\Lambda \tag{1}$$

where $n_{eff}$ is effective refractive index and period of the grating and $\Lambda$ is the period of the grating. Applying mechanical strain ($\varepsilon$) and temperature shift ($\Delta T$) cause the shift in the wavelength of the reflect light ($\Delta\lambda$). The relation between $\varepsilon$ and $\Delta\lambda_e$ (shift only by strain)is given by[10]

$$\Delta\lambda_e=\lambda_B(1-P_e)\varepsilon \tag{2}$$

where $P_e$ is the strain-optic coefficient. There are two reasons for the change in wavelength caused by temperature changes: refractive index of the optical fiber and the change in the physical length of the fiber through thermal expansion. Generally the relation between $\Delta T$ and $\Delta\lambda_T$ (shift only by temperature) is given by[10]

$$\Delta\lambda_T=\lambda_B\xi\Delta T \tag{3}$$

where $\xi$ is thermo-optic coefficient depending on the type of fiber. We can conclude that stress and temperature difference linearly change the wavelength shift.

### B. Calibration of needle deformation calculation model

In this study we embedded three fibers on the stylet of needle placed $120^\circ$ apart as Fig1. Five FBG sensors are placed along each fiber. $\lambda_B$ of the three FBGs in the same position are the same. Deformation of the needle causes the FBG to be stretched or compressed. Using the beam-column theory to get the relation between bending strain ($\varepsilon$) and relative curvature ($\kappa$) for each sensor is

$$\varepsilon=\frac{d}{\rho}=d\cdot\kappa \tag{4}$$

where $d$ is the distance between the axis of sensors and the neutral plane and $\rho$ is the radius of curvature.

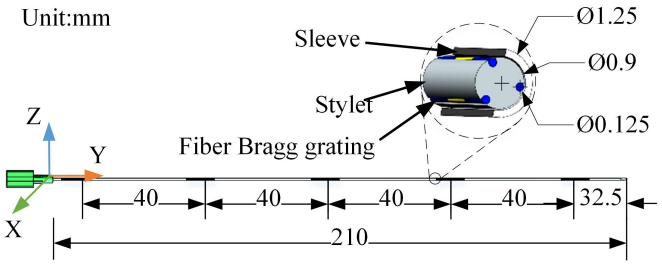


Fig. 1 Configuration of the needle with FBG sensors

Establish a right-handed coordinate system with the y-axis perpendicular to the end face of the needle base. Then the shape of the needle can be described by a spatial curve. It can be synthesized by projection of the x-y and x-z planes. The curvature of the spatial curve can also be synthesized by the curvature of the projected curves in x-y and x-z planes. So we propose a calculation model as

$$\begin{bmatrix}\Delta\lambda1\\ \Delta\lambda2\\ \Delta\lambda3\end{bmatrix}_i=\begin{bmatrix}C_1(\mathrm{xy}) & C_1(\mathrm{xz})\\ C_2(\mathrm{xy}) & C_2(\mathrm{xz})\\ C_3(\mathrm{xy}) & C_3(\mathrm{xz})\end{bmatrix}_i\begin{bmatrix}\kappa_{xy}\\ \kappa_{xz}\end{bmatrix}_i \qquad (i=1,2,3,4,5) \tag{5}$$

Where $\kappa_{xy}$ and $\kappa_{xz}$ is the relative curvature of the projected curves in x-y and x-z planes. Each set of sensors corresponds to a calibration matrix. This model does not take into account wavelength changes caused by torque applied and temperature change. Due to the split structure of the needle, the torque applied to the sleeve cannot be applied to the stylet, whether calibrated or actually used. One reason is the sleeve and stylet are relatively fixed by the external device without relative rotation. Another one is the gap between the sleeve and the stylet causes the torque is hardly transmitted to the stylet from sleeve. The reason for the insensitivity to temperature is that

the FBG of the same wavelength has the same temperature characteristics and is eliminated during the calibration matrix. If we heat a certain set of FBGs, (5) transfers to

$$\begin{bmatrix} C_1 & C_2 & C_3 \\ C_4 & C_5 & C_6 \end{bmatrix}_i = \begin{bmatrix} C_1(\mathrm{xy}) & C_1(\mathrm{xz}) \\ C_2(\mathrm{xy}) & C_2(\mathrm{xz}) \\ C_3(\mathrm{xy}) & C_3(\mathrm{xz}) \end{bmatrix}_i^{-1} \tag{6}$$

$$\begin{bmatrix} C_1 & C_2 & C_3 \\ C_4 & C_5 & C_6 \end{bmatrix}_i \left( \begin{bmatrix} \Delta\lambda 1 \\ \Delta\lambda 2 \\ \Delta\lambda 3 \end{bmatrix}_i + \begin{bmatrix} \lambda_B \xi \Delta T \\ \lambda_B \xi \Delta T \\ \lambda_B \xi \Delta T \end{bmatrix} \right) = \begin{bmatrix} \kappa_{xy} \\ \kappa_{xz} \end{bmatrix}_i \tag{7}$$

However, previous analyses have shown that the wavelength change caused by temperature is due to changes in the physical properties of the fiber material rather than the deformation of the needle. So there is no change in $\kappa_{xy}$ and $\kappa_{xz}$. We get another conclusion about calibration matrix as (8) and (9). This also proves that the calibration model is not sensitive to temperature.

$$C_1+C_2+C_3=0 \tag{8}$$

$$C_4+C_5+C_6=0 \tag{9}$$

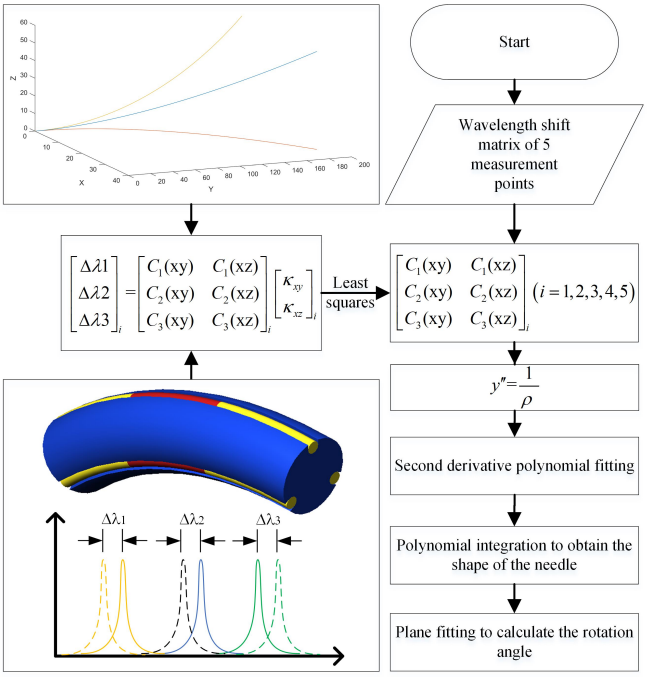


Fig. 2 Process of calibration method

The calibration method is shown in Fig 2. Our calibration method only considers the curvature in the plane. First, the theoretical curvature ( $\kappa_{xy}$ and $\kappa_{xz}$ ) corresponding to each group of FBGs and the actual measured wavelength shift are input into the calibration model at different angles. Then use the least squares method to calculate the calibration matrix. Then perform error analysis. Using the resulting matrix to calculate $\kappa_{xy}$ and $\kappa_{xz}$ for each position. The relation between curvature and the second derivative of the curve as

$$\kappa = \pm \frac{y''}{\sqrt{\left[1+(y')^2\right]^3}} \tag{10}$$

Since the needle deformation is relatively small, the second-order small amount ( $(y')^2$ ) is ignored. Using the polynomial fitting to obtain a fifth-order polynomial about the second derivative of the curve of the needle shape on the projection surface. Then integrate $y''$ twice under zero initial conditions to get the projection curve of the needle shape. Finally, the two curves are combined and fitted to the plane using least squares to calculate the deflection direction and the actual curvature.

## III. Experiments

### A. Experimental Setup

The complete experimental setup for the calibration procedure is shown in Fig.3. A calibration phantom with a series of semicircular grooves with constant radius of curvature was fabricated. The semicircular grooves are machined by CNC using a ball milling cutter. The two symmetrical stencils together can completely lock the needle in the groove to ensure that the deformation of the needle is exactly the same as the design curve. This configuration can prevent the needle from being warped and the actual deformation curve of the needle does not match the curve being processed. The needle rotates in the grooves to simulate that the needle is deformed by loads in different directions. We have designed a special clamp to secure the stylet, the sleeve and the encoder's rotary shaft to ensure a precise angle of rotation of stylet. The angular resolution of the encoder is $0.025^\circ$. Encoder housing via a connecting plate fixedly connected with the phantom using screw bolt. The size of the needle was 18G×210 mm. The inner stylet was cut by electric spark to three small grooves with a diameter of 0.165mm parallel to the central axis of the stylet, at 120 intervals. The fibers with FBG sensors were glued to the inner stylet grooves under microscope with adhesive Loctite1C-LV (Locite Corp, USA). Three fibers are connected to an Optical Sensing Instrument TV155 interrogator (Micron Optics, Inc).

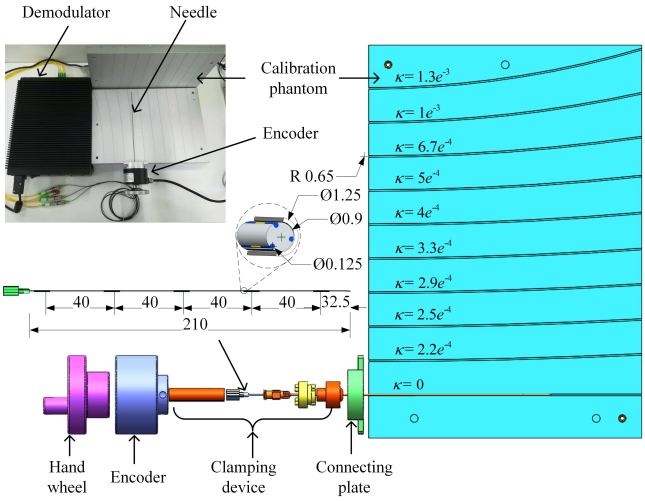


Fig. 3 Calibration experiment device

### B. *Validation of the Calculation Model*

The verification process of the calculation model is as follows.

- First we chosen $\kappa$=0 , $\kappa$=2.5$e^{-4}$ , $\kappa$=5$e^{-4}$ and $\kappa$=1.3$e^{-3}$ as the calibration curves. Needle was fixed in the groove of $\kappa$=0 and combine the two phantoms. The needle would be in an ideal straight line. Recorded the value of the encoder and the wavelengths of 15 FBGs. These would be the benchmark for the next calculation.
- Then put the needle into $\kappa$=2.5$e^{-4}$ , $\kappa$=5$e^{-4}$ and $\kappa$=1.3$e^{-3}$ as the first step. Rotate the hand wheel one turn. Record twenty angles in each groove and their corresponding wavelengths of 15 FBGs.
- Use MATLAB to calculate the curvature ( $\kappa_{xy}$ and $\kappa_{xz}$ ) of the corresponding curve projection at these angles.
- Enter all the raw data into the calibration model to find the least squares solution of the calibration matrix through MATLAB and calculate the fitted mean error.
- Finally, randomly put the needle into the other groove as in the second step and get the test data (a set of curvature angle and wavelength).

## IV. Results

In this section we first calculated the calibration matrix using the data from $\kappa$=2.5$e^{-4}$ , $\kappa$=5$e^{-4}$ and $\kappa$=1.3$e^{-3}$ . Then using the calibration matrix to analyze the fitting error of angle. Finally, the test data is used to analyze the prediction accuracy of the calibration model for curvature and angle.

The calibration matrix for each sensor location as follows.

$$C_1=\begin{bmatrix}-376.072 & -13.958\\ 100.747 & -303.181\\ 188.924 & 272.743\end{bmatrix}\quad C_1^{-1}=\begin{bmatrix}-0.00204 & 0.00081 & 0.00079\\ 0.00023 & -0.00194 & 0.00151\end{bmatrix}$$

$$C_2=\begin{bmatrix}-417.029 & -18.432\\ 147.508 & -340.915\\ 163.979 & 295.372\end{bmatrix}\quad C_2^{-1}=\begin{bmatrix}-0.00187 & 0.00071 & 0.00070\\ -0.00004 & -0.00169 & 0.00142\end{bmatrix}$$

$$C_3=\begin{bmatrix}-408.616 & -146.209\\ 211.946 & -299.551\\ 86.854 & 301.602\end{bmatrix}\quad C_3^{-1}=\begin{bmatrix}-0.00181 & 0.00113 & 0.00025\\ -0.00052 & -0.00161 & 0.00147\end{bmatrix}$$

$$C_4=\begin{bmatrix}-384.784 & -147.707\\ 154.885 & -292.479\\ 13.223 & 316.132\end{bmatrix}\quad C_4^{-1}=\begin{bmatrix}-0.00218 & 0.00104 & -0.00006\\ -0.00055 & -0.00149 & 0.00152\end{bmatrix}$$

$$C_5=\begin{bmatrix}-139.629 & -128.692\\ 99.827 & -153.272\\ 64.994 & 235.046\end{bmatrix}\quad C_5^{-1}=\begin{bmatrix}-0.00381 & 0.00425 & 0.00068\\ -0.00063 & -0.00241 & 0.00234\end{bmatrix}$$

The sum of each column in the calibration matrix is close to 0. This means that this needle with FBG sensors can only be used at a certain temperature range. The reason is that it is difficult to keep $\lambda_B$ consistent during the grating production process.

Fig4 shows the results of angle error. This error indicates the resolution of the direction of the load source with FBG sensors. The average direction error between calculated from FBG sensors and actually measured are 8.58° , 4.77° , 5.43° , 4.88° , 3.32° , 3.72° , 3.79° , 3.91° and 1.52° respectively constrained to different curvatures. The higher the resolution of the load direction as the curvature increases approximately. The standard deviation of the direction error decreases as the curvature increases. Because the FBG wavelength shift is more obvious as the curvature increases, the stronger the noise immunity.

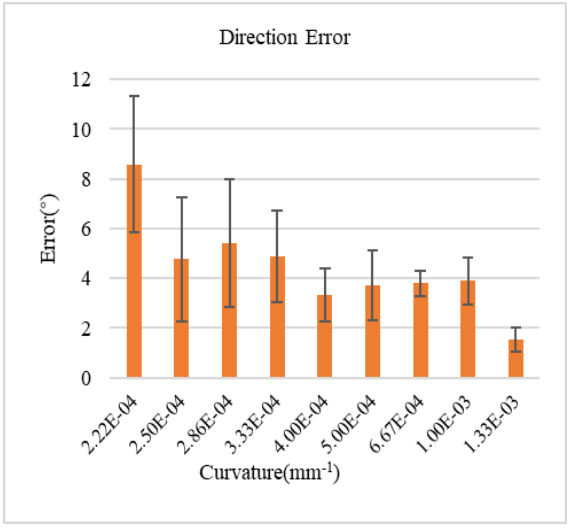


Fig.4 Experimental results for loading direction estimation

Fig 5 shows the Euclidean distance error for each sensor's location with different curvatures and different loading directions. This error indicates the accuracy of shape reconstruction. Under different curvatures, the error increases as the distance of the sensor from the needle base increases. When the load direction is constant, the error has no obvious law with the increase of the curvature, and only keeps within a certain range. The maximum error 2.36mm occurs when the curvature is 0.001mm$^{-1}$ and the loading direction is 270° .

## V. Discussion

A calibration procedure and machine for accurate needle shape reconstruction using strain measurements from FBG sensors was presented. The results show that the matrix obtained by calibration of this method can only be used at a certain temperature range due to the inevitable grating manufacturing error. Although the direction estimation error is relatively large when the curvature is small, the shape reconstruction error is not too large in small curvature, which can still meet the surgical requirements. When the curvature is relatively large, although the direction estimation error is small, the shape reconstruction error is large. However, combined with the doctor's clinical experience, the situation when the curvature is $\kappa$=1$e^{-3}$ and $\kappa$=1.3$e^{-3}$ is rare. In summary, the

proposed method can meet the clinical need for estimating the loading direction and needle deflection at a certain temperature range. Future work will improve the proposed model to further improve shape reconstruction accuracy and temperature insensitivity.

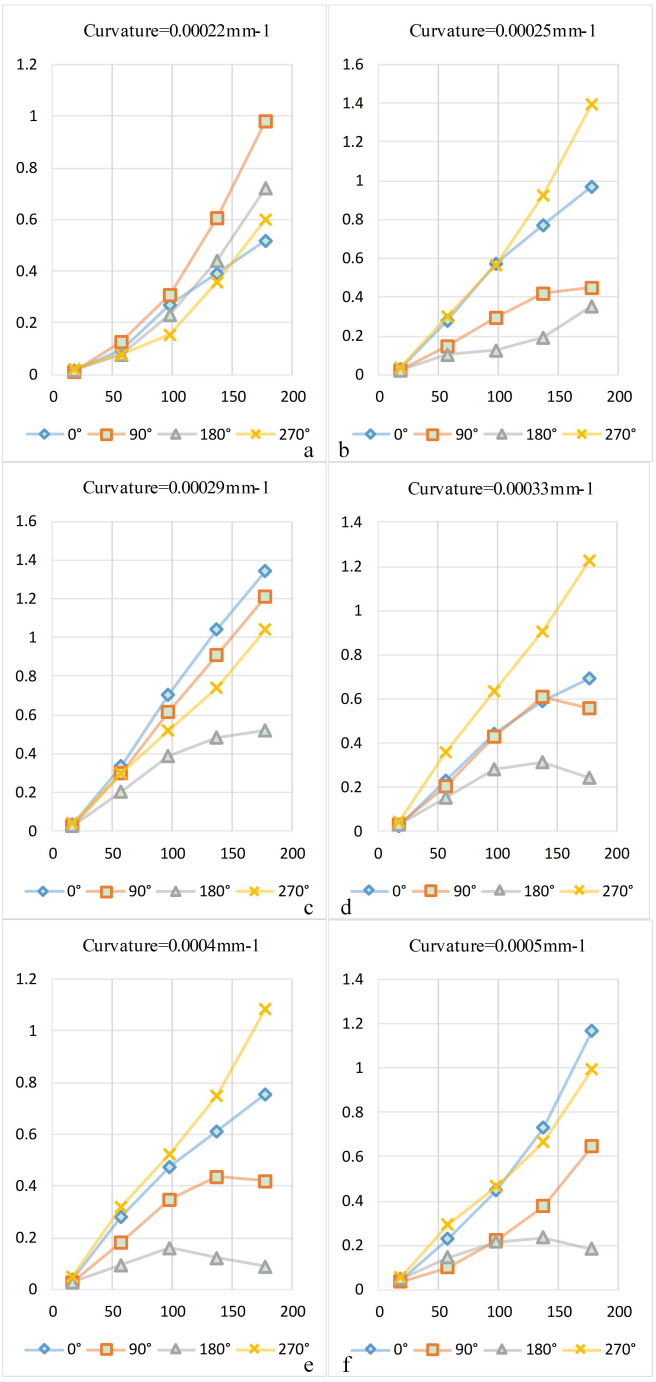


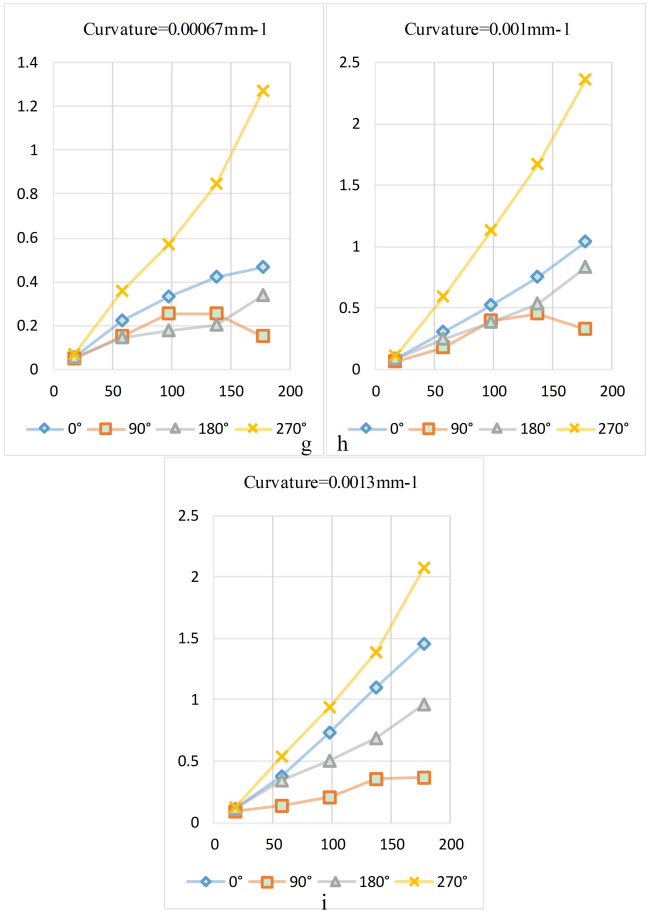


Fig.5 Experimental results for Euclidean distance error for each sensor's location

## REFERENCES


[1] T. K. Podder et al., "AAPM and GEC - ESTRO guidelines for image - guided robotic brachytherapy: Report of Task Group 192," Medical physics, vol. 41, no. 10, 2014.

[2] A. Sturdza et al., "Image guided brachytherapy in locally advanced cervical cancer: improved pelvic control and survival in RetroEMBRACE, a multicenter cohort study," Radiotherapy and Oncology, vol. 120, no. 3, pp. 428-433, 2016.

[3] A. Melzer et al., "Innomotion for percutaneous image-guided interventions," IEEE Engineering in Medicine and Biology Magazine, vol. 27, no. 3, pp. 66-73, 2008.

[4] D. Stoianovici et al., "AcuBot: a robot for radiological interventions," IEEE Transactions on Robotics and Automation, vol. 19, no. 5, pp. 927-930, 2003.

[5] J.-H. Zhu, J. Wang, Y.-G. Wang, M. Li, X.-J. Liu, and C.-B. Guo, "Prospect of robotic assistance for fully automated brachytherapy seed placement into skull base: Experimental validation in phantom and cadaver," Radiotherapy and Oncology, 2017.

[6] R. J. Webster, N. J. Cowan, G. Chirikjian, and A. M. Okamura, "Nonholonomic Modeling of Needle Steering," International Journal of Robotics Research, vol. 25, no. 5-6, pp. 509-525, 2006.

[7] N. Abolhassani and R. V. Patel, "Deflection of a flexible needle during insertion into soft tissue," in International Conference of the IEEE Engineering in Medicine & Biology Society, 2006.

[8] H. Kataoka, T. Washio, M. Audette, and K. Mizuhara, "A model for relations between needle deflection, force, and thickness on needle

penetration," in International Conference on Medical Image Computing and Computer-Assisted Intervention, 2001, pp. 966-974: Springer.

[9] C. Shi et al., "Shape Sensing Techniques for Continuum Robots in Minimally Invasive Surgery: A Survey," IEEE Transactions on Biomedical Engineering, vol. 64, no. 8, pp. 1665-1678, 2017.

[10] R. Kashyap, Fiber bragg gratings. Academic press, 2009.

[11] Y. L. Park et al., "Real-Time Estimation of 3-D Needle Shape and Deflection for MRI-Guided Interventions," IEEE Asme Trans Mechatron, vol. 15, no. 6, pp. 906-915, 2010.

[12] K. R. Henken, J. Dankelman, J. J. V. D. Dobbelsteen, L. K. Cheng, and M. S. V. D. Heiden, "Error Analysis of FBG-Based Shape Sensors for Medical Needle Tracking," IEEE/ASME Transactions on Mechatronics, vol. 19, no. 5, pp. 1523-1531, 2014.

[12] M. Abayazid, M. Kemp, and S. Misra, "3D flexible needle steering in soft-tissue phantoms using Fiber Bragg Grating sensors," in IEEE International Conference on Robotics & Automation, 2013.

[13] S. K. Jin, J. Guo, M. Chatrasingh, S. Kim, and I. Iordachita, "Shape determination during needle insertion With curvature measurements," in IEEE/RSJ International Conference on Intelligent Robots & Systems, 2017.

[14] R. J. Roesthuis, M. Kemp, J. J. V. D. Dobbelsteen, and S. Misra, "Three-Dimensional Needle Shape Reconstruction Using an Array of Fiber Bragg Grating Sensors," IEEE/ASME Transactions on Mechatronics, vol. 19, no. 4, pp. 1115-1126, 2014.

[15] Borot de Battisti, Maxence, et al. "Fiber Bragg gratings ‐ based sensing for real ‐ time needle tracking during MR ‐ guided brachytherapy." Medical physics 43.10 (2016): 5288-5297.